

# Eringen's nonlocal elasticity theory for wave propagation analysis of magneto-electro-elastic nanotubes

Farzad Ebrahimi\*, M. Dehghan and Ali Seyfi

Department of Mechanical Engineering, Faculty of Engineering, Imam Khomeini International University, Qazvin, Iran

(Received September 22, 2018, Revised November 30, 2018, Accepted December 6, 2018)

**Abstract.** In this article, wave propagation characteristics in magneto-electro-elastic (MEE) nanotube considering shell model is studied in the framework nonlocal theory. To account for the small-scale effects, the Eringen's nonlocal elasticity theory of is applied. Nonlocal governing equations of MEE nanotube have been derived utilizing Hamilton's principle. The results of this investigation have been accredited by comparing them of previous studies. An analytical solution of governing equations is used to obtain phase velocities and wave frequencies. The influences of different parameters, such as different mode, nonlocal parameter, length parameter, geometry, magnetic field and electric field on wave propagation responses of MEE nanotube are expressed in detail.

**Keywords:** wave propagation; magneto-electro-elastic nanotube; nonlocal strain gradient elasticity theory; shell model

## 1. Introduction

Magneto-electro-elastic (MEE) owing to special capability such as converting of different forms of energy have received remarkable attentions in recent researches. When they are subjected to mechanical stresses, they can make magnetic-electric coupling effects and contrariwise (Nan 1994, Spaldin and Fiebig 2005, Eerenstein *et al.* 2006). In other word these material have reciprocal reactions against mechanical and magneto electric loadings. These newfound materials are the compound of piezo-electric phases and piezo-magnetic phases and this compound causes to converting energy. Given such characteristics these types of materials can be used in different technological applications including sensors, controllers and actuators applications, robotics, medical instruments and etc. As experimental researches in nano-size are difficult, the theoretical analysis, including continuum mechanics and atomistic simulations, are becoming more momentous. On the other hand molecular dynamic simulations are complicated and time-consuming (Chowdhury *et al.* 2010, 2011). So many researchers applied continuum mechanics in order to investigate nanomaterial's mechanical behavior. In these investigations, it is very important to take into regard the small-scale influences in the mechanical analysis. Therefore size-dependent continuum theories, such as nonlocal elasticity theory (Eringen 1972, 1983) and strain gradient theory (Yang *et al.* 2002), are expanded to consider the small-scale effect (Reddy 2007, Li *et al.* 2016, 2018, Ebrahimi *et al.* 2016a, Ebrahimi and Salari 2015).

In last two decades, numerous researchers explored on vibration, bending, wave propagation and buckling behaviors of MEE nanostructures. However, some investigations were performed in recent years; Wu and Tsai (2010) examined three-dimensional free vibration response of simply supported, doubly curved magneto-electro-elastic functionally graded (MEE-FG) shells with closed-circuit surface conditions using the perturbation method. Nonlinear vibration behavior of magneto-electro-thermo-elastic nanobeams exposed to external electric voltage, external magnetic potential and uniform temperature rise is presented by Ansari *et al.* (2015). Shooshtari and Razavi (2015) studied nonlinear and linear free vibration of symmetrically laminated MEE doubly-curved thin shell resting on an elastic foundation. Ebrahimi and Barati (2016) discussed the buckling characteristics of MEE-FG nanoplates resting on Winkler–Pasternak foundation using nonlocal four-variable refined plate theory. Wave propagation analysis of a MEE-FG nanobeam subjected to axial load based upon classical beam theory is carried out by Ebrahimi *et al.* (2016b). Results indicate that the magnetic or electric nanostructures analysis is of great significance. In other work, Ebrahimi and Dabbagh (2017a) analyzed wave propagation behavior of smart rotating MEE-FG nanoplates in the framework of nonlocal strain gradient theory (NSGT). Free vibration and biaxial buckling characteristics of double MEE nanoplates systems exposed to initial external electric and magnetic potentials, using nonlocal plate theory is performed by Jamalpoor *et al.* (2017). Arefi and Zenkour (2017) explored wave propagation answers of MEE-FG nanobeam with rectangular cross section rest on visco-Pasternak foundation utilizing Timoshenko beam model. Wave dispersion of MEE nanobeam via Euler nanobeam model and Timoshenko nanobeam model is reported by (Ma *et al.* 2017). Size-dependent continuum model is developed by Farajpour *et*

\* Corresponding author, Ph.D., Professor,  
E-mail: febrahimi@eng.ikiu.ac.ir

*al.* (2017) to examine the nonlinear buckling of MEE hybrid nanoshells in thermal environment. Ebrahimi and Dabbagh (2017b) further studied wave propagation characteristics of smart MEE-FG nanoplates based on NSGT. Since the structural element of nanotubes is more like to the cylindrical shell, a suitable model in considering these characteristics must be taken into account. Hence, in order to attain more precise results, the use of shell model has attracted the consideration of many researchers (Ansari *et al.* 2015). Besides some scientists employed shell theories to analyze different issues. For example, wave propagation analysis of carbon nanotubes (CNTs) with elastic Euler-Bernoulli and Timoshenko beam models is surveyed by Wang (2005). Liew and Wang (2007) investigated wave propagation in both single-walled carbon nanotubes (SWCNTs) and double-walled carbon nanotubes (DWCNTs) via two developed elastic shell theories: Love's thin cylindrical shell theory and the Cooper–Naghdi thick cylindrical shell theory. The transverse and torsional wave in SWCNTs and DWCNTs, focusing on the efficacy of carbon nanotube microstructure on wave dispersion and the SWCNTs and DWCNTs are modeled as nonlocal single and double elastic cylindrical shells is studied by (Hu *et al.* 2008). Plus, Gürses *et al.* (2009) examined free vibration behavior of laminated skew plates using discrete singular convolution (DSC) technique in the framework of first-order shear deformation theory. Moreover, Baltacıoğlu *et al.* (2010) presented bending analysis of laminated composite plates using DSC method based on first-order shear deformation theory (FSDT). In other study, Baltacıoğlu *et al.* (2011) investigated nonlinear static characteristics of a laminated rectangular plate resting on nonlinear elastic foundation with cubic nonlinearity in the framework of FSDT. In addition, buckling response of SWCNT based upon modified strain gradient elasticity and modified couple stress theories is carried out by Akgöz and Civalek (2011). Euler-Bernoulli beam model is developed by Civalek and Demir (2011) to analyze the bending and buckling behaviors of cantilever CNT based on nonlocal elasticity theory of Eringen. Axial buckling response of double-walled boron nitride nanotubes (BNNTs) embedded in an elastic medium under combined electro-thermo-mechanical loadings is performed by (Arani *et al.* 2012) using nonlocal cylindrical piezoelectricity continuum shell theory. A novel efficient method to evaluate the bending analysis of a non-uniform Bernoulli–Euler beam resting on an elastic winker foundation is presented by Tsiatas (2014). Mercan and Civalek (2016) studied buckling analysis of BNNT surrounded by an elastic matrix utilizing DSC method and Euler–Bernoulli beam model. Thereafter, surface effect on stability analysis of Silicon carbide nanotubes (SiCNTs) considering nonlocal elasticity using the harmonic differential quadrature (HDQ) method is performed by Mercan and Civalek (2017). Ehyaei and Daman (2017) analyzed free vibration characteristics of DWCNTs resting on an elastic medium regarding initial imperfection. Free vibration response of bi-directional functionally graded (FG) nanobeams with Euler-Bernoulli beam theory is discussed by Nejad *et al.* (2017). Zhu and Li (2017d) studied twisting static responses of through-radius

FG nanotubes in the framework of Eringen's nonlocal integral elasticity. In another research, Zhu and Li (2017b) examined size influence of longitudinal and torsional dynamic behavior of small-scaled rods are modeled by utilizing an integral formula of two-phase nonlocal theory. A size-dependent integral elasticity model is developed for a rod with small-scale in stress based upon the NSGT is investigated by Zhu and Li (2017a). Also, Zhu and Li (2017c) performed the longitudinal dynamic analysis of a size-dependent elasticity rod by using an integral form of NSGT. Kheibari and Beni (2017) explored size effect on free vibration of piezoelectric nanotubes based on Love's cylindrical thin-shell model by using consistent couple stress theory. Vibration analysis of embedded SWCNTs considering initial thermal loading effects based on the nonlocal shell model by applying variational differential quadrature method is reported by Ansari *et al.* (2018). Mohammadi *et al.* (2018) examined vibration behavior and instability of SWCNT conveying viscous fluid using molecular dynamics simulation in the framework of nonlocal strain gradient cylindrical shell model. Free and transient vibration analysis of composite laminated open cylindrical shells with general boundary conditions using a simple first-order shear deformation shell theory is analyzed by Wang *et al.* (2018). Ke *et al.* (2014) studied the size-dependent vibration of embedded MEE cylindrical nanoshells in the framework of the nonlocal theory and Love's thin shell theory. Zeighampour *et al.* (2017) discussed wave propagation in DWCNT fluid-conveying due to the slip boundary condition and shell model based on the NSGT. Size effect on nonlinear buckling and postbuckling characteristics of MEE cylindrical composite nanoshells is carried out by Sahmani and Aghdam (2018). Ebrahimi and Dabbagh (2018) studied wave propagation analysis of rotating heterogeneous MEE nanobeams considering external magnetic and electric fields based on NSGT. Wave propagation response of MEE nanoshells via two nonlocal strain gradient shell theories; the Kirchhoff–Love shell theory and the first-order shear deformation shell theory is discussed by Ma *et al.* (2018). Kamali *et al.* (2018) examined postbuckling behavior of smart MEE composite nanotubes resting on a nonlinear elastic foundation in a non-uniform thermal environment. The buckling behavior of MEE nanobeams based on of the Euler-Bernoulli beam model with the von Kármán geometrical nonlinearity using the modified couple stress theory subjected to different thermal loading and electric and magnetic fields is reported by Alibeigi *et al.* (2018). Ghorbanpour-Arani *et al.* (2018) investigated buckling analysis of an embedded MEE sandwich nanoplate based on a nonlocal magneto-electro-elasticity theory using refined zigzag theory.

To date, it is obvious that there is not any investigation on the wave propagation behavior of a MEE nanotube considering shell model in the framework of nonlocal theory. Present paper demonstrates a new probing on wave propagation analysis of MEE-FG nanotube considering shell model based on nonlocal theory. In addition to considering the small size effects, the nonlocal elasticity theory is employed here. Hamilton's principle is employed to extend the nonlocal governing equations of MEE

nanotube. After deriving the governing equations, the wave propagation problem is presented for a nanotube. Using an exponential wave propagation solution, the dispersion relations between the phase velocity and wave number are derived. Eventually, influences of different parameters on the wave propagation responses of MEE-FG nanotube are discussed.

## 2. Theory and formulation

### 2.1 Nonlocal theory for MEE materials

This theory can be extended to MEEMs taking into account the elastic, magnetic and electric field (Ke *et al.* 2014). So that elastic, magnetic and electric field for a reference point belong not only on the strain components, magnetic and electric induction at the same point but also on all other points of the MEE body. The basic equations for MEE cylinder nanoshell can be expressed as follows (Ke *et al.* 2014)

$$(1-(e_0a)^2\nabla^2)\begin{Bmatrix} \sigma_x \\ \sigma_\theta \\ \sigma_{x\theta} \end{Bmatrix} = \begin{bmatrix} \tilde{c}_{11} & \tilde{c}_{12} & 0 \\ \tilde{c}_{21} & \tilde{c}_{22} & 0 \\ 0 & 0 & c_{66} \end{bmatrix} \begin{Bmatrix} \varepsilon_x \\ \varepsilon_\theta \\ \gamma_{x\theta} \end{Bmatrix} - \begin{bmatrix} 0 & 0 & \tilde{e}_{31} \\ 0 & 0 & \tilde{e}_{32} \\ 0 & 0 & 0 \end{bmatrix} \begin{Bmatrix} E_x \\ E_\theta \\ E_z \end{Bmatrix} - \begin{bmatrix} 0 & 0 & \tilde{q}_{31} \\ 0 & 0 & \tilde{q}_{32} \\ 0 & 0 & 0 \end{bmatrix} \begin{Bmatrix} H_x \\ H_\theta \\ H_z \end{Bmatrix} - \begin{bmatrix} \beta_1 \\ \beta_1 \\ 0 \end{bmatrix} \Delta T \quad (1)$$

$$(1-(e_0a)^2\nabla^2)\begin{Bmatrix} D_x \\ D_\theta \\ D_z \end{Bmatrix} = \begin{bmatrix} 0 & 0 & 0 \\ 0 & 0 & 0 \\ \tilde{e}_{31} & \tilde{e}_{32} & 0 \end{bmatrix} \begin{Bmatrix} \varepsilon_x \\ \varepsilon_\theta \\ \gamma_{x\theta} \end{Bmatrix} - \begin{bmatrix} \tilde{s}_{11} & 0 & 0 \\ 0 & \tilde{s}_{22} & 0 \\ 0 & 0 & \tilde{s}_{33} \end{bmatrix} \begin{Bmatrix} E_x \\ E_\theta \\ E_z \end{Bmatrix} - \begin{bmatrix} \tilde{d}_{11} & 0 & 0 \\ 0 & \tilde{d}_{22} & 0 \\ 0 & 0 & \tilde{d}_{33} \end{bmatrix} \begin{Bmatrix} H_x \\ H_\theta \\ H_z \end{Bmatrix} + \begin{bmatrix} 0 \\ 0 \\ p_3 \end{bmatrix} \Delta T \quad (2)$$

$$(1-(e_0a)^2\nabla^2)\begin{Bmatrix} B_x \\ B_\theta \\ B_z \end{Bmatrix} = \begin{bmatrix} 0 & 0 & 0 \\ 0 & 0 & 0 \\ \tilde{q}_{31} & \tilde{q}_{32} & 0 \end{bmatrix} \begin{Bmatrix} \varepsilon_x \\ \varepsilon_\theta \\ \gamma_{x\theta} \end{Bmatrix} - \begin{bmatrix} \tilde{d}_{11} & 0 & 0 \\ 0 & \tilde{d}_{22} & 0 \\ 0 & 0 & \tilde{d}_{33} \end{bmatrix} \begin{Bmatrix} E_x \\ E_\theta \\ E_z \end{Bmatrix} - \begin{bmatrix} \tilde{\mu}_{11} & 0 & 0 \\ 0 & \tilde{\mu}_{22} & 0 \\ 0 & 0 & \tilde{\mu}_{33} \end{bmatrix} \begin{Bmatrix} H_x \\ H_\theta \\ H_z \end{Bmatrix} + \begin{bmatrix} 0 \\ 0 \\ \lambda_3 \end{bmatrix} \Delta T \quad (3)$$

In these equations  $e_0a$ ,  $\Delta T$  are nonlocal parameter and temperature difference, respectively;

$$\nabla^2 = \frac{\partial}{\partial R^2} + \frac{1}{R} \frac{\partial}{\partial R} + \frac{1}{R^2} \frac{\partial^2}{\partial \theta^2} + \frac{\partial^2}{\partial z^2}.$$

The three dimensional stress state reduced constants for the MEE cylindrical nanoshell are as follows

$$\begin{aligned} \tilde{c}_{11} &= c_{11} - \frac{c_{13}^2}{c_{33}}, & \tilde{c}_{12} &= c_{12} - \frac{c_{13}^2}{c_{33}}, \\ \tilde{c}_{66} &= c_{66}, & \tilde{e}_{66} &= e_{66}, \\ \tilde{e}_{31} &= e_{31} - \frac{c_{13}e_{33}}{c_{33}}, & \tilde{q}_{31} &= q_{31} - \frac{c_{13}q_{33}}{c_{33}}, \\ \tilde{s}_{11} &= s_{11}, & \tilde{s}_{33} &= s_{33} - \frac{e_{33}^2}{c_{33}}, \\ \tilde{d}_{11} &= d_{11}, & \tilde{d}_{33} &= d_{33} + \frac{q_{33}e_{33}}{c_{33}}, \\ \tilde{\beta}_1 &= \beta_1 - \frac{c_{13}\beta_3}{c_{33}}, & \tilde{p}_3 &= p_3 + \frac{\beta_3e_{33}}{c_{33}}, \\ \tilde{\lambda}_3 &= \lambda_3 + \frac{\beta_3q_{33}}{c_{33}}, & \tilde{\mu}_{11} &= \mu_{11}, \\ \tilde{\mu}_{33} &= \mu_{33} - \frac{q_{33}^2}{c_{33}} \end{aligned} \quad (4)$$

where

$$\{A_{11}, A_{12}, A_{66}\} = \{\tilde{c}_{11}h, \tilde{c}_{12}h, \tilde{c}_{66}h\} \quad (5)$$

$$\{D_{11}, D_{12}, D_{66}\} = \left\{ \frac{\tilde{c}_{11}h^3}{12}, \frac{\tilde{c}_{12}h^3}{12}, \frac{\tilde{c}_{66}h^3}{12} \right\} \quad (6)$$

$$\{E_{31}, Q_{31}\} = \int_{-h/2}^{h/2} \{\tilde{e}_{31}, \tilde{q}_{31}\} \beta \sin(\beta z) dz \quad (7)$$

$$X_{11} = \int_{-h/2}^{h/2} \tilde{s}_{11} \cos^2(\beta z) dz \quad (8)$$

$$X_{22} = \int_{-h/2}^{h/2} \tilde{s}_{11} \left[ \frac{\cos(\beta z)}{R+z} \right]^2 dz \quad (9)$$

$$X_{33} = \int_{-h/2}^{h/2} \tilde{s}_{33} [\beta \sin(\beta z)]^2 dz \quad (10)$$

$$Y_{11} = \int_{-h/2}^{h/2} \tilde{d}_{11} \cos^2(\beta z) dz \quad (11)$$

$$Y_{22} = \int_{-h/2}^{h/2} \tilde{d}_{22} \left[ \frac{\cos(\beta z)}{R+z} \right]^2 dz \quad (12)$$

$$X_{33} = \int_{-h/2}^{h/2} \tilde{d}_{33} [\beta \sin(\beta z)]^2 dz \quad (13)$$

$$T_{11} = \int_{-h/2}^{h/2} \tilde{\mu}_{11} \cos^2(\beta z) dz \quad (14)$$

Table 1 Properties of magneto-electro-elastic material  
BiTiO<sub>3</sub>, CoFe<sub>2</sub>O<sub>4</sub>

Properties	BiTiO <sub>3</sub> – CoFe <sub>2</sub> O <sub>4</sub>
Elastic (GPa)	$c_{11} = 226, c_{12} = 125,$ $c_{13} = 124, c_{33} = 216,$ $c_{44} = 44.2, c_{66} = 50.5$
Piezoelectric (cm <sup>2</sup> )	$e_{31} = -2.2,$ $e_{33} = 9.3, e_{15} = 5.8$
Dielectric (10 <sup>-9</sup> C Vm <sup>-1</sup> )	$s_{11} = 5.64, s_{33} = 6.35$
Piezomagnetic (N Am <sup>-1</sup> )	$q_{15} = 275,$ $q_{31} = 290.1, q_{33} = 349.9$
Magnetoelastic (10 <sup>-12</sup> Ns VC <sup>-1</sup> )	$d_{11} = 5.367, d_{33} = 2737.5$
Magnetic (10 <sup>-6</sup> Ns <sup>2</sup> C <sup>-2</sup> )	$\mu_{11} = -297, \mu_{31} = 83.5$
Thermal Moduli (10 <sup>5</sup> NKm <sup>-2</sup> )	$\beta_1 = 4.74, \beta_3 = 4.53$
Pyroelectric (10 <sup>-6</sup> CN <sup>-1</sup> )	$p_3 = 25$
Pyromagnetic (10 <sup>-6</sup> NAmK <sup>-1</sup> )	$\lambda_3 = 5.19$
Mass Density (10 <sup>3</sup> Kg m <sup>-3</sup> )	$\rho = 5.55$

$$T_{22} = \int_{-h/2}^{h/2} \tilde{\mu}_{22} \left[ \frac{\cos(\beta z)}{R+z} \right]^2 dz \quad (15)$$

$$T_{33} = \int_{-h/2}^{h/2} \tilde{\mu}_{33} [\beta \sin(\beta z)]^2 dz \quad (16)$$

The constants of the material properties used in this study are presented in Table 1.

Also, in these equations the electric field is defined as follows

$$E_x = -\frac{\partial \tilde{\Phi}}{\partial x} = \cos(\beta z) \frac{\partial \Phi}{\partial x} \quad (17)$$

$$E_\theta = -\frac{1}{R+z} \frac{\partial \tilde{\Phi}}{\partial \theta} = \frac{\cos(\beta z)}{R+z} \frac{\partial \Phi}{\partial \theta} \quad (18)$$

$$E_z = -\frac{\partial \tilde{\Phi}}{\partial z} = -\beta \sin(\beta z) \Phi - \frac{2\phi_0}{h} \quad (19)$$

And the magnetic field can be defined as follows

$$H_x = -\frac{\partial \tilde{\Psi}}{\partial x} = \cos(\beta z) \frac{\partial \Psi}{\partial x} \quad (20)$$

$$H_\theta = -\frac{1}{R+z} \frac{\partial \tilde{\Psi}}{\partial \theta} = \frac{\cos(\beta z)}{R+z} \frac{\partial \Psi}{\partial \theta} \quad (21)$$

$$H_z = -\frac{\partial \tilde{\Psi}}{\partial z} = -\beta \sin(\beta z) \Psi - \frac{2\psi_0}{h} \quad (22)$$

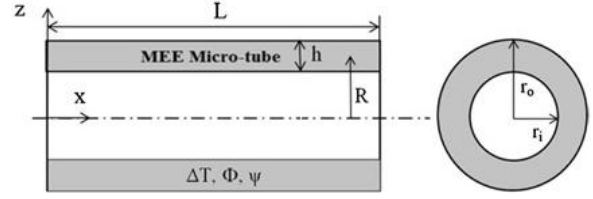


Fig. 1 Schematic view MEE nanotube model

In general, the electrical and magnetic potentials are obtained from the following equations

$$\Phi(x, \theta, z, t) = -\cos(\beta z) \Phi(x, \theta, t) + \frac{2z\phi_0}{h} \quad (23)$$

$$\Psi(x, \theta, z, t) = -\cos(\beta z) \Psi(x, \theta, t) + \frac{2z\psi_0}{h} \quad (24)$$

In this equation  $\beta = \frac{\pi}{h}$ ;  $\Phi(x, \theta, t)$  and  $\Psi(x, \theta, t)$  the spatial variation of the electric potential and magnetic potential in the  $x$  and  $\theta$  directions. also,  $\phi_0$  and  $\psi_0$  are the initial external electric potential and magnetic potential, respectively.

## 2.2 Cylinder nanoshell

In Fig. 1 Schematic configuration of a MEE cylindrical nanoshell model is provided nasldianotube with length of  $L$ , radius of  $R$  and thickness of  $h$  that is assumed to be subjected to an electric potential field  $\tilde{\Phi}(x, \theta, z, t)$  and a magnetic potential field  $\tilde{\Psi}(x, \theta, z, t)$ . According to nonlocal Love's shell theory. The displacement field is assumed to be

$$u_x(x, \theta, z, t) = U(x, \theta, t) + z \frac{\partial W(x, \theta, t)}{\partial x} \quad (25)$$

$$u_\theta(x, \theta, z, t) = U(x, \theta, t) + z \frac{\partial W(x, \theta, t)}{\partial \theta} \quad (26)$$

$$u_z(x, \theta, z, t) = W(x, \theta, t) \quad (27)$$

Based on Love's shell theory, the strain-displacement relations can be expressed in terms of the mid-plane strains and curvatures as follows

$$\varepsilon_x = \frac{\partial U}{\partial x} - z \frac{\partial^2 W}{\partial x^2} \quad (28)$$

$$\varepsilon_\theta = \frac{1}{R} \left( \frac{\partial V}{\partial \theta} + W \right) - \frac{z}{R^2} \left( \frac{\partial^2 W}{\partial \theta^2} - \frac{\partial V}{\partial \theta} \right) \quad (29)$$

$$\gamma_{x\theta} = \frac{\partial V}{\partial x} + \frac{1}{R} \frac{\partial U}{\partial \theta} - \frac{z}{R} \left( \frac{\partial^2 W}{\partial x \partial \theta} - \frac{\partial V}{\partial x} \right) \quad (30)$$

Normal forces  $\{N_x, N_\theta, N_{x\theta}\}$  and bending moment can be written as follow

$$\{N_x, N_\theta, N_{x\theta}\} = \int_{-h/2}^{h/2} \{\sigma_x, \sigma_\theta, \sigma_{x\theta}\} dz \quad (31)$$

$$\{M_x, M_\theta, M_{x\theta}\} = \int_{-h/2}^{h/2} \{\sigma_x, \sigma_\theta, \sigma_{x\theta}\} z dz \quad (32)$$

By substituting Eqs. (17)-(32) into Eqs. (1), (2), (3) the following equations can be obtained

$$N_x - \mu^2 \nabla^2 N_x = A_{11} \frac{\partial U}{\partial x} + \frac{A_{12}}{R} \left( \frac{\partial V}{\partial \theta} + W \right) + N_{Mx} + N_{Ex} + N_{Tx} \quad (33)$$

$$N_\theta - \mu^2 \nabla^2 N_\theta = A_{12} \frac{\partial U}{\partial x} + \frac{A_{11}}{R} \left( \frac{\partial V}{\partial \theta} + W \right) + N_{M\theta} + N_{E\theta} + N_{T\theta} \quad (34)$$

$$N_{x\theta} - e_0 a^2 \nabla^2 N_{x\theta} = A_{66} \left( \frac{\partial V}{\partial x} + \frac{1}{R} \frac{\partial U}{\partial \theta} \right) \quad (35)$$

$$M_x - e_0 a^2 \nabla^2 M_x = -D_{11} \frac{\partial^3 W}{\partial x^2} - \frac{D_{12}}{R^2} \left( \frac{\partial^3 W}{\partial \theta^2} - \frac{\partial V}{\partial \theta} \right) + E_{31} \Phi + Q_{31} \Psi \quad (36)$$

$$M_\theta - e_0 a^2 \nabla^2 M_\theta = -D_{12} \frac{\partial^3 W}{\partial x^2} - \frac{D_{11}}{R^2} \left( \frac{\partial^3 W}{\partial \theta^2} - \frac{\partial V}{\partial \theta} \right) + E_{31} \Phi + Q_{31} \Psi \quad (37)$$

$$M_{x\theta} - e_0 a^2 \nabla^2 M_{x\theta} = -\frac{D_{66}}{R} \left( \frac{2}{R} \frac{\partial^3 W}{\partial \theta \partial x} - \frac{\partial V}{\partial x} \right) \quad (38)$$

$$\int_{-h/2}^{h/2} \cos(\beta z) \left[ D_x - e_0 a^2 \nabla^2 D_x \right] dz = X_{11} \frac{\partial \Phi}{\partial x} + Y_{11} \frac{\partial \Psi}{\partial x} \quad (39)$$

$$\int_{-h/2}^{h/2} \frac{\cos(\beta z)}{R+z} \left[ D_\theta - e_0 a^2 \nabla^2 D_\theta \right] dz = X_{22} \frac{\partial \Phi}{\partial \theta} + Y_{22} \frac{\partial \Psi}{\partial \theta} \quad (40)$$

$$\int_{-h/2}^{h/2} \beta \sin(\beta z) \left[ D_z - e_0 a^2 \nabla^2 D_z \right] dz = -E_{31} \frac{\partial^3 W}{\partial x^2} - \frac{E_{31}}{R^2} \left( \frac{\partial^3 W}{\partial \theta^2} - \frac{\partial V}{\partial \theta} \right) - X_{33} \Phi - Y_{33} \Psi + E_{31} \left( \frac{1}{R^4} \frac{\partial^4 W}{\partial \theta^4} + \frac{1}{R^2} \frac{\partial^3 W}{\partial x^2 \partial \theta^2} - \frac{1}{R^4} \frac{\partial^3 V}{\partial \theta^3} - \frac{1}{R^2} \frac{\partial^3 V}{\partial x^2 \partial \theta} \right) \quad (41)$$

### 2.3 Obtaining the governing equations

Hamilton's principle expresses that total variational derivation of kinetic and potential energies and work done By non-potential forces In time interval  $\Delta t = t_2 - t_1$  is zero.

Considering the Hamilton's principle

$$\int_{t_1}^{t_2} \delta(\Pi_k - (\Pi_F + \Pi_S)) dt = 0 \quad (42)$$

Where  $\Pi_S$  stands for total strain energy,  $\Pi_K$  is kinetic energy,  $\Pi_F$  is work done by external force.

#### 2.3.1 Strain energy

Total strain energy equals to consequent  $\Pi_{s1}$  elastic strain energy,  $\Pi_{s2}$  electric strain energy and  $\Pi_{s3}$  magnetic strain energy.

$$\Pi_s = \Pi_{s1} + \Pi_{s2} + \Pi_{s3} \quad (43)$$

$$\Pi_{s1} = \frac{1}{2} \int_0^L \int_0^{2\pi} \left[ N_x \frac{\partial U}{\partial x} + \frac{N_\theta}{R} \left( \frac{\partial V}{\partial \theta} + W \right) + N_{x\theta} \left( \frac{\partial V}{\partial x} + \frac{1}{R} \frac{\partial U}{\partial \theta} \right) \right] R d\theta dx - \frac{1}{2} \int_0^L \int_0^{2\pi} \left[ M_x \frac{\partial^2 W}{\partial x^2} + \frac{M_\theta}{R^2} \left( \frac{\partial^2 W}{\partial \theta^2} - \frac{\partial V}{\partial \theta} \right) + \frac{M_{x\theta}}{R} \left( \frac{2\partial^2 W}{\partial x \partial \theta} - \frac{\partial V}{\partial x} \right) \right] R d\theta dx \quad (44)$$

$$\Pi_{s2} = -\frac{1}{2} \int_0^L \int_0^{2\pi} \int_{-h/2}^{h/2} \left[ D_x \cos(\beta z) \frac{\partial \Phi}{\partial x} + D_\theta \frac{\cos(\beta z)}{R+z} \frac{\partial \Phi}{\partial \theta} - D_z (\beta \sin(\beta z)) \Phi + \frac{2\psi_0}{h} \right] R dz d\theta dx \quad (45)$$

$$\Pi_{s3} = -\frac{1}{2} \int_0^L \int_0^{2\pi} \int_{-h/2}^{h/2} \left[ B_x \cos(\beta z) \frac{\partial \Psi}{\partial x} + B_\theta \frac{\cos(\beta z)}{R+z} \frac{\partial \Psi}{\partial \theta} - B_z (\beta \sin(\beta z)) \Psi + \frac{2\psi_0}{h} \right] R dz d\theta dx \quad (46)$$

#### 2.3.2 Kinetic energy

Kinetic energy of nanotube can be expressed as

$$\Pi_k = \frac{1}{2} \int_0^L \int_0^{2\pi} \left[ I_1 \left( \frac{\partial U}{\partial t} \right)^2 + I_1 \left( \frac{\partial V}{\partial t} \right)^2 + I_1 \left( \frac{\partial W}{\partial t} \right)^2 \right] R d\theta dx \quad (47)$$

in which  $I_1 = \rho h$ .

#### 2.3.3 Work of external force

The external force actually is electric and magnetic field of nanotube that work done by them is defined as

$$\Pi_F = \frac{1}{2} \int_0^L \int_0^{2\pi} \left[ (N_{Ex} + N_{Mx} + N_{Tx}) \left( \frac{\partial W}{\partial t} \right)^2 \right] R d\theta dx + \quad (48)$$

$$\frac{1}{2} \int_0^L \int_0^{2\pi} \left[ \frac{(N_{E\theta} + N_{M\theta} + N_{T\theta})}{R^2} \left( \frac{\partial W}{\partial \theta} \right)^2 \right] R d\theta dx$$

where  $(N_{Ex}, N_{E\theta}), (N_{Mx}, N_{M\theta})$  are vertical forces induced by external electric potential  $\phi_0$  and external magnetic potential  $\psi_0$  in  $x$ - $\theta$  directions which are defined as follows

$$N_{Tx} = N_{T\theta} = \tilde{\beta}_1 h \Delta T, \quad N_{Ex} = N_{E\theta} = -2\tilde{e}_{31} \phi_0, \quad N_{Mx} = N_{M\theta} = -2\tilde{q}_{31} \psi_0 \quad (49)$$

By substituting above equations in Hamilton's principle

$\int_0^t (\delta \Pi_k - (\delta \Pi_F + \delta \Pi_G + \delta \Pi_S)) dt = 0$  the governing equations of the MEE nanoshell can be obtained

$$\delta U : \frac{\partial N_x}{\partial x} + \frac{1}{R} \frac{\partial N_{x\theta}}{\partial \theta} = I_1 \frac{\partial^2 U}{\partial t^2} \quad (50)$$

$$\delta V: \frac{\partial N_{x\theta}}{\partial x} + \frac{1}{R} \frac{\partial N_\theta}{\partial \theta} + \frac{1}{R} \frac{\partial M_{x\theta}}{\partial x} + \frac{1}{R^2} \frac{\partial M_\theta}{\partial \theta} = I_1 \frac{\partial^2 V}{\partial t^2} \quad (51)$$

$$\delta W: \frac{\partial M_x}{\partial x^2} + \frac{2}{R} \frac{\partial^2 M_{x\theta}}{\partial x \partial \theta} + \frac{1}{R^2} \frac{\partial^2 M_\theta}{\partial \theta^2} - \frac{N_\theta}{R} - N_{x0} \frac{\partial^2 W}{\partial x^2} - \frac{N_{\theta 0}}{R^2} \frac{\partial^2 W}{\partial \theta^2} = I_1 \frac{\partial^2 W}{\partial t^2} \quad (52)$$

$$\delta \Phi: \int_{-h/2}^{h/2} \left[ \frac{\partial D_x}{\partial x} \cos(\beta z) + \frac{\cos(\beta z)}{R+z} \frac{\partial D_\theta}{\partial \theta} + D_z \beta \sin(\beta z) \right] dz = 0 \quad (53)$$

$$\delta \Psi: \int_{-h/2}^{h/2} \left[ \frac{\partial B_x}{\partial x} \cos(\beta z) + \frac{\cos(\beta z)}{R+z} \frac{\partial B_\theta}{\partial \theta} + B_z \beta \sin(\beta z) \right] dz = 0 \quad (54)$$

in these equation  $N_{x0} = N_{Ex} + N_{Mx}$  and  $N_{\theta 0} = N_{E\theta} + N_{M\theta}$ .

By substituting Eqs. (33)-(41) into Eqs. (50)-(54) governing equations of problem can be found as follows

$$A_{11} \frac{\partial^2 U}{\partial x^2} + \frac{A_{12}}{R} \left( \frac{\partial^3 V}{\partial x \partial \theta} + \frac{\partial W}{\partial x} \right) + \frac{A_{66}}{R} \frac{\partial^3 V}{\partial x \partial \theta} + \frac{A_{66}}{R^2} \frac{\partial^2 U}{\partial \theta^2} = \{1 - e_0 a^2 \nabla^2\} (I_1 \frac{\partial^2 U}{\partial t^2}) \quad (55)$$

$$A_{66} \frac{\partial^3 V}{\partial x^2} + \frac{A_{66}}{R} \frac{\partial^2 U}{\partial x \partial \theta} - \frac{A_{12}}{R} \frac{\partial^2 U}{\partial x \partial \theta} + \frac{A_{11}}{R^2} \frac{\partial^3 V}{\partial \theta^2} + \frac{A_{11}}{R^2} \frac{\partial W}{\partial \theta} - \frac{D_{66}}{R^2} \frac{2 \partial^3 W}{\partial x^2 \partial \theta^2} + \frac{D_{66}}{R^2} \frac{\partial^3 V}{\partial x^2} - \frac{D_{12}}{R^2} \frac{\partial^3 W}{\partial x^2 \partial \theta} - \frac{D_{11}}{R^4} \frac{\partial^3 W}{\partial \theta^3} + \frac{D_{11}}{R^4} \frac{\partial^3 V}{\partial \theta^2} + \frac{E_{31}}{R^2} \frac{\partial \Phi}{\partial \theta} + \frac{Q_{31}}{R^2} \frac{\partial \Psi}{\partial \theta} = \{1 - e_0 a^2 \nabla^2\} (I_1 \frac{\partial^3 V}{\partial t^2}) \quad (56)$$

$$-D_{11} \frac{\partial^4 W}{\partial x^4} - \frac{D_{12}}{R^2} \frac{\partial^3 W}{\partial x^2 \partial \theta^2} + \frac{D_{12}}{R^2} \frac{\partial^3 V}{\partial x^2 \partial \theta} + E_{31} \frac{\partial^2 \Phi}{\partial x^2} + Q_{31} \frac{\partial^2 \Psi}{\partial x^2} + \frac{4D_{66}}{R^2} \frac{\partial^3 W}{\partial x^2 \partial \theta^2} + \frac{2D_{66}}{R^2} \frac{\partial^3 V}{\partial x^2 \partial \theta} - \frac{D_{12}}{R^2} \frac{\partial^3 W}{\partial x^2 \partial \theta^2} - \frac{D_{11}}{R^4} \frac{\partial^3 W}{\partial \theta^4} + \frac{D_{11}}{R^4} \frac{\partial^3 V}{\partial \theta^3} + \frac{E_{31}}{R^2} \frac{\partial^2 \Phi}{\partial \theta^2} + \frac{Q_{31}}{R^2} \frac{\partial^2 \Psi}{\partial \theta^2} - \frac{A_{12}}{R} \frac{\partial U}{\partial x} - \frac{A_{11}}{R^2} \frac{\partial V}{\partial \theta} - \frac{A_{11} W}{R^2} + \frac{N_{E\theta}}{R} + \frac{N_{M\theta}}{R} = \{1 - e_0 a^2 \nabla^2\} \left( \frac{N_{\theta 0}}{R^2} \frac{\partial^3 W}{\partial \theta^2} + N_{x0} \frac{\partial^3 W}{\partial x^2} + I_1 \frac{\partial^3 W}{\partial t^2} \right) \quad (57)$$

$$X_{11} \frac{\partial^2 \Phi}{\partial x^2} + Y_{11} \frac{\partial^2 \Psi}{\partial x^2} + X_{22} \frac{\partial^2 \Phi}{\partial \theta^2} + Y_{22} \frac{\partial^2 \Psi}{\partial \theta^2} - E_{31} \frac{\partial^3 W}{\partial x^2} - \frac{E_{31}}{R^2} \frac{\partial^3 W}{\partial \theta^2} + \frac{E_{31}}{R^2} \frac{\partial V}{\partial \theta} - X_{33} \Phi - Y_{33} \Psi + Y_{33} I^2 \frac{\partial^2 \Psi}{\partial x^2} = 0 \quad (58)$$

$$Y_{11} \frac{\partial^2 \Phi}{\partial x^2} + T_{11} \frac{\partial^2 \Psi}{\partial x^2} + Y_{22} \frac{\partial^2 \Phi}{\partial \theta^2} + T_{22} \frac{\partial^2 \Psi}{\partial \theta^2} - Q_{31} \frac{\partial^3 W}{\partial x^2} - \frac{Q_{31}}{R^2} \frac{\partial^3 W}{\partial \theta^2} + \frac{Q_{31}}{R^2} \frac{\partial V}{\partial \theta} - Y_{33} \Phi - T_{33} \Psi = 0 \quad (59)$$

### 3. Solving the equation

For solving wave propagation equation obtained, instead of parameters  $U, V, W, \Phi, \Psi$ ; following expressions placed in the equation and the equation obtained to be placed in matrix separately.

$$\begin{bmatrix} u \\ v \\ w \\ \varphi \\ \psi \end{bmatrix} = \begin{bmatrix} \bar{U} e^{i(kx+m\theta-\omega t)} \\ \bar{V} e^{i(kx+m\theta-\omega t)} \\ \bar{W} e^{i(kx+m\theta-\omega t)} \\ \bar{\varphi} e^{i(kx+m\theta-\omega t)} \\ \bar{\psi} e^{i(kx+m\theta-\omega t)} \end{bmatrix} \quad (60)$$

The resulting matrix is formed as follows

$$\begin{bmatrix} K_{11} - M_{11}\omega^2 & K_{12} & K_{13} & K_{14} & K_{15} \\ K_{21} & K_{22} - M_{22}\omega^2 & K_{23} & K_{24} & K_{25} \\ K_{31} & K_{32} & K_{33} - M_{33}\omega^2 & K_{34} & K_{35} \\ K_{41} & K_{42} & K_{43} & K_{44} - M_{44}\omega^2 & K_{45} \\ K_{51} & K_{52} & K_{53} & K_{54} & K_{55} - M_{55}\omega^2 \end{bmatrix} \begin{bmatrix} U \\ V \\ W \\ \Phi \\ \Psi \end{bmatrix} = 0 \quad (61)$$

where the element of matrix are listed in Appendix 1. The nontrivial solution of equation gives the natural frequency and wave velocity can be calculated by following relation

$$c = \frac{\omega}{k} \quad (61)$$

### 4. Results and discussion

Hu *et al.* (2008) investigated nonlocal effect wave propagation in carbon nanotube using Flugge cylinder shell theory and also, Verified own results with Molecular dynamics. Obtained results from this study is consistent with obtained results in Hu investigation completely.

In order to compare present study and study of reference dimensionless frequency of both studies calculated and compared with each other. In present study dimensionless

frequency is  $\Omega = \omega L \sqrt{\frac{I_1}{A_{11}}}$ .

As observed in Fig. 2 almost in the wave numbers lower than 2 (1/nm) of local theory and nonlocal theory yields same results but higher than this wave number the amount of dimensionless frequency for local theory with  $e_0 = 0.6$  is less than result of nonlocal theory. In Hu *et al.* (2008) obtained results via nonlocal theory is compatible with obtained results of molecular dynamics.

#### 4.1 Different mode on phase velocity

Fig. 3 shows the chart of phase velocity versus wave number in different vibrational modes for  $m = 1$ . Results indicates that range of wave number 0.01 – 0.1 (1/nm) amount of phase velocity by rising mode number enlarges but in range of 0.1 – 1 (1/nm) first mode has maximum velocity and is higher than other modes. For range 1 (1/nm) all modes leads to a same value.

#### 4.2 The effect of nonlocal parameter on phase velocity

Variations of phase velocity and wave frequency versus different wave number is presented in Table 2. In this table three nonlocal parameters 0, 0.5, 1 (nm) have been compared each other. When nonlocal parameter equal to zero, actually responses are equivalent to response of classical theory. As can be seen in smaller wave number the amount of phase velocity and wave frequency in different parameters are almost close to each other and it can be concluded that classical and nonlocal theories have same results in small wave numbers but in wave numbers higher than  $1 \times 10^9$  (1/m), classical theory results it is very different. The reason of the difference between the results is that in

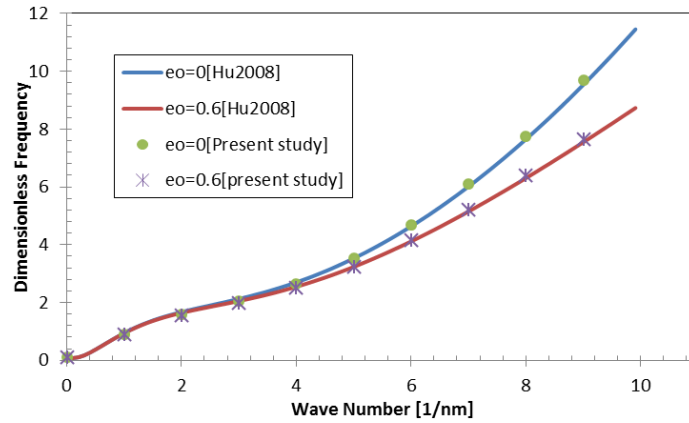


Fig. 2 The chart of dimensionless versus wave number compare with (Hu *et al.* 2008)

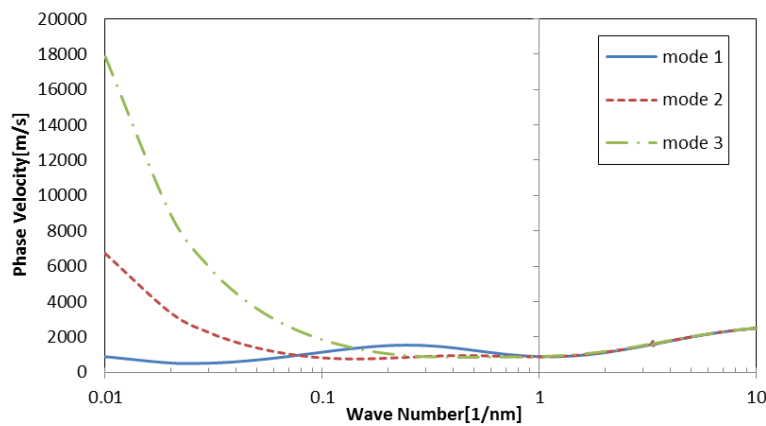


Fig. 3 The chart of phase velocity versus wave number in different vibration modes

Table 2 Variations of phase velocity and wave frequency versus wave number with nonlocal parameters.  $m = 1, l = 1$

$e_0\alpha$ (nm)	Wave number (1/nm)	Phase velocity (Km/s)	Wave frequency (THz)
0	0.1	1.13783	0.114219
0	1	0.907245	0.907245
0	5	2.82394	14.1197
0	50	3.01775	150.888
0.5	0.1	1.13783	0.113783
0.5	1	0.809179	0.809179
0.5	5	1.0494	5.24698
0.5	50	1.10416	55.3408
1	0.1	1.12505	0.112505
1	1	0.637466	0.637466
1	5	0.555986	2.77993
1	50	0.555696	27.7848

nonlocal theory, properties of a point are not considered as properties of that specific point but these properties are related to all points of the body.

Fig. 4 illustrates the variations of phase velocity versus wave number with different nonlocal parameters. In this

figure, three nonlocal parameters 0, 0.2, 0.5, 1 (nm) have been compared to each other. As can be seen, at first all chart have same value and in this range occurred a peak then after  $1 \times 10^9$  (1/m) the charts are slightly spaced apart and in wave number  $1 \times 10^9$  (1/m) classical theory present quite upward chart and in  $5 \times 10^9$  become constant. Phase velocity is reduced with increasing of nonlocal parameter and this reduction because of by rising this parameter continuum of material is assumed and more smooth structure results in material.

#### 4.3 The effect of geometry on phase velocity

Fig. 5 show phase velocity versus wave number in different geometric ratios. In this chart for all three modes radius to thickness 10, 20, 50 is drawn. Maximum amount of phase velocity for smaller geometric ratios occurred in bigger wave number. By rising radius to thickness ratio material rigidity is decreased and owing to it phase velocity will be smaller.

#### 4.4 The effect of magnetic field on phase velocity

Changes of phase velocity versus wave number in various magnetic field intensities is presented in Fig. 6. Generally influences of magnetic field in lower wave number can be observed and for higher wave number phase velocities are same. As seen, if magnetic field intensity is

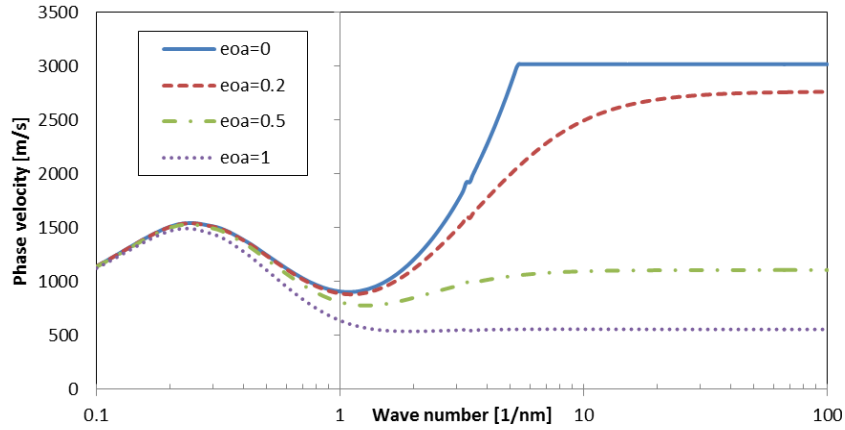


Fig. 4 The chart of variations of phase velocity versus wave number with different nonlocal parameters.  $m = 1, l = 1$

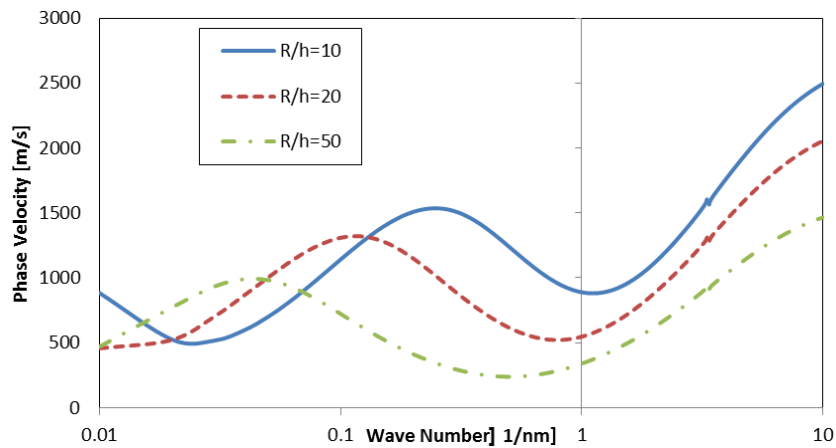


Fig. 5 The chart of phase velocity versus wave number in different geometric ratios  $L = 10$  nm

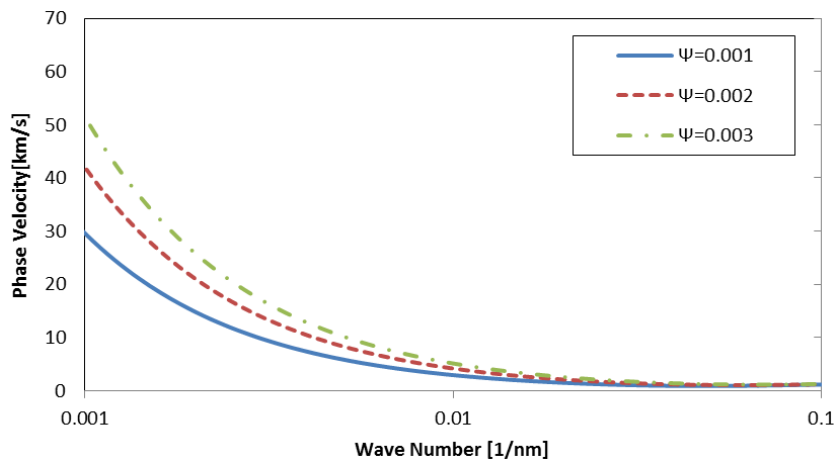


Fig. 6 The chart of phase velocity versus wave number in magnetic field with different intensities

increased, phase velocity is increased too. The reason of this behavior is that MEE material has the ability to absorb magnetism and keep it and by rising magnetic field intensity, this ability shows own more. This material capable to convert force of magnetic potential to mechanical force. Hence by rising field intensity phase velocity enlarges because magnetic field creates tensile force in nanotube.

#### 4.5 The effect of electric field on phase velocity

In Fig. 7 variations of phase velocity versus wave number in different electric field values 0.0005, 0.001, 0.002, 0.003 Volt is shown. As can be observed, for higher wave number 0.1 (1/nm) changes of electric field has not any effect on phase velocity but in lower wave number by rising electric field, phase velocity is reduced. For 0.0005,

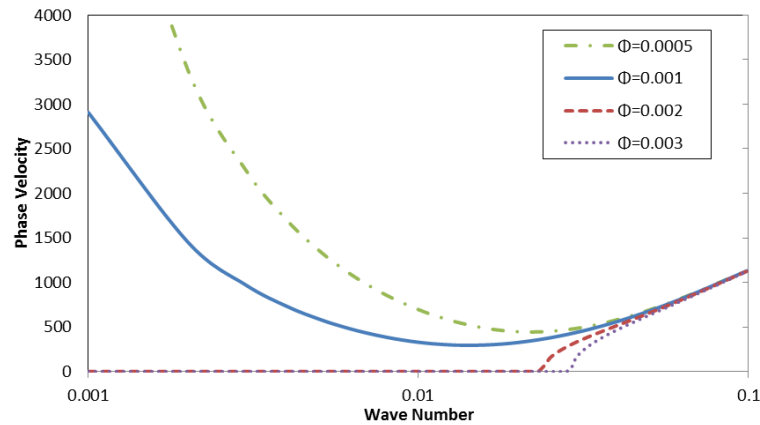


Fig. 7 The chart of variations of phase velocity versus wave number in different electric field intensities,  $\Psi = 0$

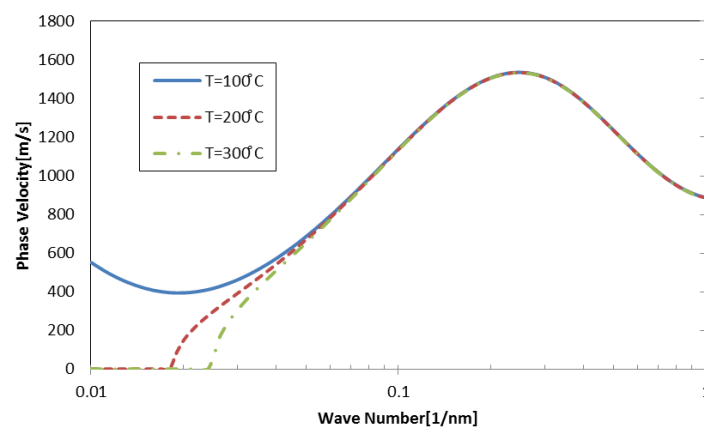


Fig. 8 The chart of variation of phase velocity versus wave number for different thermal fields

0.001 volt phase velocity is descending at first then is ascending. Critical wave numbers for 0.002, 0.003 volt are 0.024, 0.029 (1/nm), respectively and phase velocities are 60.8, 35.6, respectively.

#### 4.6 The effect of thermal field on phase velocity

Variation of phase velocity versus wave number in different thermal fields by temperature difference 100, 200, 300 ( $^{\circ}\text{C}$ ) is presented in Fig. 8. One in 100 ( $^{\circ}\text{C}$ ) there is not critical phase velocity. Also, in 100 ( $^{\circ}\text{C}$ ), chart has downtrend then has uptrend and then downtrend. But trends of other thermal fields at first is ascending and then is descending. Critical phase velocity is occurred in almost wave number 0.1 (1/nm) and after this point all thermal fields have same value. In lower wave number, by rising temperature difference, phase velocity is decreased because temperature increasing causes reduction of material rigidity.

## 5. Conclusions

In this research analytic results of wave propagation in magneto-electro-elastic nanotube using nonlocal theory and cylindrical shell theory was investigated. The effect length parameter and nonlocal parameter and effect of variation of them was examined and also the effect of aspect ratio,

magnetic field, electric field on wave propagation in MEE nanotube was investigated. Obtained results indicates as:

- By rising nonlocal parameter, phase velocity decreases.
- By rising magnetic field intensity, phase velocity increases.
- By rising electric field intensity, phase velocity decreases in lower wave number.
- By reversing electric field direction, increasing field intensity, phase velocity would be increased.
- In low wave number by rising thermal field, phase velocity is reduced

## References

- Akgöz, B. and Civalek, Ö. (2011), "Buckling analysis of cantilever carbon nanotubes using the strain gradient elasticity and modified couple stress theories", *J. Computat. Theor. Nanosci.*, **8**(9), 1821-1827.
- Alibeigi, B., Beni, Y.T. and Mehralian, F. (2018), "On the thermal buckling of magneto-electro-elastic piezoelectric nanobeams", *Eur. Phys. J. Plus*, **133**(3), 133.
- Ansari, R., Gholami, R. and Rouhi, H. (2015), "Size-dependent nonlinear forced vibration analysis of magneto-electro-thermo-elastic Timoshenko nanobeams based upon the nonlocal elasticity theory", *Compos. Struct.*, **126**, 216-226.
- Ansari, R., Torabi, J. and Faghieh Shojaei, M. (2018), "An efficient

- numerical method for analyzing the thermal effects on the vibration of embedded single-walled carbon nanotubes based on the nonlocal shell model”, *Mech. Adv. Mater. Struct.*, **25**(6), 500-511.
- Arani, A.G., Amir, S., Shajari, A. and Mozdianfard, M. (2012), “Electro-thermo-mechanical buckling of DWBNNTs embedded in bundle of CNTs using nonlocal piezoelectricity cylindrical shell theory”, *Compos. Part B: Eng.*, **43**(2), 195-203.
- Arefi, M. and Zenkour, A.M. (2017), “Wave propagation analysis of a functionally graded magneto-electro-elastic nanobeam rest on Visco-Pasternak foundation”, *Mech. Res. Commun.*, **79**, 51-62.
- Baltacıoğlu, A.K., Akgöz, B. and Civalek, Ö. (2010), “Nonlinear static response of laminated composite plates by discrete singular convolution method”, *Compos. Struct.*, **93**(1), 153-161.
- Baltacıoğlu, A., Civalek, Ö., Akgöz, B. and Demir, F. (2011), “Large deflection analysis of laminated composite plates resting on nonlinear elastic foundations by the method of discrete singular convolution”, *Int. J. Press. Vessels Pip.*, **88**(8-9), 290-300.
- Chowdhury, R., Adhikari, S., Wang, C. and Scarpa, F. (2010), “A molecular mechanics approach for the vibration of single-walled carbon nanotubes”, *Computat. Mater. Sci.*, **48**(4), 730-735.
- Chowdhury, R., Adhikari, S. and Scarpa, F. (2011), “Vibration of ZnO nanotubes: a molecular mechanics approach”, *Appl. Phys. A*, **102**(2), 301-308.
- Civalek, Ö. and Demir, C. (2011), “Buckling and bending analyses of cantilever carbon nanotubes using the euler-bernoulli beam theory based on non-local continuum model”, *Asian J. Civil Eng.*, **12**(5), 651-661.
- Ebrahimi, F. and Barati, M.R. (2016), “Static stability analysis of smart magneto-electro-elastic heterogeneous nanoplates embedded in an elastic medium based on a four-variable refined plate theory”, *Smart Mater. Struct.*, **25**(10), 105014.
- Ebrahimi, F. and Dabbagh, A. (2017a), “Nonlocal strain gradient based wave dispersion behavior of smart rotating magneto-electro-elastic nanoplates”, *Mater. Res. Express*, **4**(2), 025003.
- Ebrahimi, F. and Dabbagh, A. (2017b), “On flexural wave propagation responses of smart FG magneto-electro-elastic nanoplates via nonlocal strain gradient theory”, *Compos. Struct.*, **162**, 281-293.
- Ebrahimi, F. and Dabbagh, A. (2018), “Wave dispersion characteristics of rotating heterogeneous magneto-electro-elastic nanobeams based on nonlocal strain gradient elasticity theory”, *J. Electromagnet. Waves Applicat.*, **32**(2), 138-169.
- Ebrahimi, F. and Salari, E. (2015), “Nonlocal thermo-mechanical vibration analysis of functionally graded nanobeams in thermal environment”, *Acta Astronautica*, **113**, 29-50.
- Ebrahimi, F., Barati, M.R. and Dabbagh, A. (2016a), “A nonlocal strain gradient theory for wave propagation analysis in temperature-dependent inhomogeneous nanoplates”, *Int. J. Eng. Sci.*, **107**, 169-182.
- Ebrahimi, F., Barati, M.R. and Dabbagh, A. (2016b), “Wave dispersion characteristics of axially loaded magneto-electro-elastic nanobeams”, *Appl. Phys. A*, **122**(11), 949.
- Eerenstein, W., Mathur, N. and Scott, J.F. (2006), “Multiferroic and magnetoelectric materials”, *Nature*, **442**(7104), 759-765.
- Ehyaeei, J. and Daman, M. (2017), “Free vibration analysis of double walled carbon nanotubes embedded in an elastic medium with initial imperfection”, *Adv. Nano Res., Int. J.*, **5**(2), 179-192.
- Eringen, A.C. (1972), “Linear theory of nonlocal elasticity and dispersion of plane waves”, *Int. J. Eng. Sci.*, **10**(5), 425-435.
- Eringen, A.C. (1983), “On differential equations of nonlocal elasticity and solutions of screw dislocation and surface waves”, *J. Appl. Phys.*, **54**(9), 4703-4710.
- Farajpour, A., Rastgoo, A. and Farajpour, M. (2017), “Nonlinear buckling analysis of magneto-electro-elastic CNT-MT hybrid nanoshells based on the nonlocal continuum mechanics”, *Compos. Struct.*, **180**, 179-191.
- Ghorbanpour-Arani, A., Kolahdouzan, F. and Abdollahian, M. (2018), “Nonlocal buckling of embedded magneto-electro-elastic sandwich nanoplate using refined zigzag theory”, *Appl. Math. Mech.*, **39**(4), 529-546.
- Gürses, M., Civalek, Ö., Korkmaz, A.K. and Ersoy, H. (2009), “Free vibration analysis of symmetric laminated skew plates by discrete singular convolution technique based on first-order shear deformation theory”, *Int. J. Numer. Methods Eng.*, **79**(3), 290-313.
- Hu, Y.-G., Liew, K.M., Wang, Q., He, X. and Yakobson, B. (2008), “Nonlocal shell model for elastic wave propagation in single- and double-walled carbon nanotubes”, *J. Mech. Phys. Solids*, **56**(12), 3475-3485.
- Jamalpoor, A., Ahmadi-Savadkoobi, A., Hosseini, M. and Hosseini-Hashemi, S. (2017), “Free vibration and biaxial buckling analysis of double magneto-electro-elastic nanoplate-systems coupled by a visco-Pasternak medium via nonlocal elasticity theory”, *Eur. J. Mech.-A/Solids*, **63**, 84-98.
- Kamali, M., Shamsi, M. and Saidi, A. (2018), “Postbuckling of magneto-electro-elastic CNT-MT composite nanotubes resting on a nonlinear elastic medium in a non-uniform thermal environment”, *Eur. Phys. J. Plus*, **133**(3), 110.
- Ke, L., Wang, Y. and Reddy, J. (2014), “Thermo-electro-mechanical vibration of size-dependent piezoelectric cylindrical nanoshells under various boundary conditions”, *Compos. Struct.*, **116**, 626-636.
- Kheibari, F. and Beni, Y.T. (2017), “Size dependent electro-mechanical vibration of single-walled piezoelectric nanotubes using thin shell model”, *Mater. Des.*, **114**, 572-583.
- Li, L., Li, X. and Hu, Y. (2016), “Free vibration analysis of nonlocal strain gradient beams made of functionally graded material”, *Int. J. Eng. Sci.*, **102**, 77-92.
- Li, L., Tang, H. and Hu, Y. (2018), “The effect of thickness on the mechanics of nanobeams”, *Int. J. Eng. Sci.*, **123**, 81-91.
- Liew, K.M. and Wang, Q. (2007), “Analysis of wave propagation in carbon nanotubes via elastic shell theories”, *Int. J. Eng. Sci.*, **45**(2-8), 227-241.
- Ma, L.-H., Ke, L.-L., Wang, Y.-Z. and Wang, Y.-S. (2017), “Wave propagation in magneto-electro-elastic nanobeams via two nonlocal beam models”, *Phys. E: Low-dimensional Syst. Nanostruct.*, **86**, 253-261.
- Ma, L., Ke, L., Reddy, J., Yang, J., Kitipornchai, S. and Wang, Y. (2018), “Wave propagation characteristics in magneto-electro-elastic nanoshells using nonlocal strain gradient theory”, *Compos. Struct.*, **199**, 10-23.
- Mercan, K. and Civalek, Ö. (2016), “DSC method for buckling analysis of boron nitride nanotube (BNNT) surrounded by an elastic matrix”, *Compos. Struct.*, **143**, 300-309.
- Mercan, K. and Civalek, Ö. (2017), “Buckling analysis of Silicon carbide nanotubes (SiCNTs) with surface effect and nonlocal elasticity using the method of HDQ”, *Compos. Part B: Eng.*, **114**, 34-45.
- Mohammadi, K., Rajabpour, A. and Ghadiri, M. (2018), “Calibration of nonlocal strain gradient shell model for vibration analysis of a CNT conveying viscous fluid using molecular dynamics simulation”, *Computat. Mater. Sci.*, **148**, 104-115.
- Nan, C.-W. (1994), “Magneto-electric effect in composites of piezoelectric and piezomagnetic phases”, *Phys. Rev. B*, **50**(9), 6082.
- Nejad, M.Z., Hadi, A. and Farajpour, A. (2017), “Consistent couple-stress theory for free vibration analysis of Euler-Bernoulli nano-beams made of arbitrary bi-directional

- functionally graded materials”, *Struct. Eng. Mech., Int. J.*, **63**(2), 161-169.
- Reddy, J. (2007), “Nonlocal theories for bending, buckling and vibration of beams”, *Int. J. Eng. Sci.*, **45**(2-8), 288-307.
- Sahmani, S. and Aghdam, M. (2018), “Nonlocal strain gradient shell model for axial buckling and postbuckling analysis of magneto-electro-elastic composite nanoshells”, *Compos. Part B: Eng.*, **132**, 258-274.
- Shooshtari, A. and Razavi, S. (2015), “Linear and nonlinear free vibration of a multilayered magneto-electro-elastic doubly-curved shell on elastic foundation”, *Compos. Part B: Eng.*, **78**, 95-108.
- Spaldin, N.A. and Fiebig, M. (2005), “The renaissance of magneto-electric multiferroics”, *Science*, **309**(5733), 391-392.
- Tsiatas, G.C. (2014), “A new efficient method to evaluate exact stiffness and mass matrices of non-uniform beams resting on an elastic foundation”, *Arch. Appl. Mech.*, **84**(5), 615-623.
- Wang, Q. (2005), “Wave propagation in carbon nanotubes via nonlocal continuum mechanics”, *J. Appl. Phys.*, **98**(12), 124301.
- Wang, Q., Shao, D. and Qin, B. (2018), “A simple first-order shear deformation shell theory for vibration analysis of composite laminated open cylindrical shells with general boundary conditions”, *Compos. Struct.*, **184**, 211-232.
- Wu, C.-P. and Tsai, Y.-H. (2010), “Dynamic responses of functionally graded magneto-electro-elastic shells with closed-circuit surface conditions using the method of multiple scales”, *Eur. J. Mech.-A/Solids*, **29**(2), 166-181.
- Yang, F., Chong, A., Lam, D.C.C. and Tong, P. (2002), “Couple stress based strain gradient theory for elasticity”, *Int. J. Solids Struct.*, **39**(10), 2731-2743.
- Zeighampour, H., Beni, Y.T. and Karimipour, I. (2017), “Wave propagation in double-walled carbon nanotube conveying fluid considering slip boundary condition and shell model based on nonlocal strain gradient theory”, *Microfluidics Nanofluidics*, **21**(5), 85.
- Zhu, X. and Li, L. (2017a), “Closed form solution for a nonlocal strain gradient rod in tension”, *Int. J. Eng. Sci.*, **119**, 16-28.
- Zhu, X. and Li, L. (2017b), “Longitudinal and torsional vibrations of size-dependent rods via nonlocal integral elasticity”, *Int. J. Mech. Sci.*, **133**, 639-650.
- Zhu, X. and Li, L. (2017c), “On longitudinal dynamics of nanorods”, *Int. J. Eng. Sci.*, **120**, 129-145.
- Zhu, X. and Li, L. (2017d), “Twisting statics of functionally graded nanotubes using Eringen's nonlocal integral model”, *Compos. Struct.*, **178**, 87-96.

CC

## Appendix 1

$$\begin{aligned}
K_{11} &= -A_{11}k^2 - \frac{A_{66}}{R^2}n^2 \\
K_{12} &= -\frac{A_{12}}{R}kn - \frac{A_{66}}{R}kn \\
K_{13} &= +\frac{A_{12}}{R}ki \\
K_{14} &= 0 \\
K_{15} &= 0 \\
K_{21} &= \frac{A_{66}}{R}kn - \frac{A_{12}}{R}kn \\
K_{22} &= -A_{66}k^2 - \frac{A_{11}}{R^2}n^2 - \frac{D_{66}}{R^2}k^2 - \frac{D_{11}}{R^4}n^2 \\
K_{23} &= +\frac{A_{11}}{R^2}ni + 2\frac{D_{66}}{R^2}k^2ni + \frac{D_{12}}{R^2}k^2ni + \frac{D_{11}}{R^4}n^3i \\
K_{24} &= \frac{E_{31}}{R^2}ni \\
K_{25} &= \frac{Q_{31}}{R^2}ni \\
K_{31} &= -\frac{A_{12}}{R}ki \\
K_{32} &= +\frac{D_{12}}{R^2}k^2ni + \frac{2D_{66}}{R^2}k^2ni - \frac{D_{11}}{R^4}n^3i - \frac{A_{11}}{R^2}ni \\
K_{33} &= -D_{11}k^4 - 2\frac{D_{12}}{R^2}k^2n^2 - \frac{4D_{66}}{R^2}k^2n^2 - \frac{D_{11}}{R^4}n^4 - \frac{A_{11}}{R^2}W + \frac{N_{\theta 0}}{R^2}n^2 + \\
&N_{x0}k^2 + (e_0a)^2\left(\frac{N_{\theta 0}}{R^4}n^4 + \frac{N_{\theta 0}}{R^2}k^2n^2 + N_{x0}k^4 + \frac{N_{x0}}{R^2}k^2n^2\right) \\
K_{34} &= -E_{31}k^2 + \frac{E_{31}}{R^2}n^2 \\
K_{35} &= -Q_{31}k^2 - \frac{Q_{31}}{R^2}n^2 \\
K_{41} &= 0 \\
K_{42} &= \frac{E_{31}}{R^2}ni \\
K_{43} &= E_{31}k^2 + \frac{E_{31}}{R^2}n^2 \\
K_{44} &= -X_{11}k^2 - X_{22}n^2 - X_{33} - X_{33}k^2 - X_{33}\frac{n^2}{R^2} \\
K_{45} &= -Y_{11}k^2 - Y_{22}n^2 \\
K_{51} &= 0 \\
K_{52} &= \frac{Q_{31}}{R^2}ni \\
K_{53} &= Q_{31}k^2 \\
K_{54} &= -Y_{11}k^2 - Y_{22}n^2 - Y_{33} \\
K_{55} &= -T_{11}k^2 - T_{22}n^2 - T_{33} \\
M_{11} &= M_{22} = M_{33} = -I_1 - I_1(e_0a)^2\left(k^2 + \frac{n^2}{R^2}\right)
\end{aligned}$$